HAL
open science

The Impact of Lithology on Fjord Morphology

Mathieu Bernard, Philippe Steer, Kerry Gallagher, D. L Egholm

To cite this version:

Mathieu Bernard, Philippe Steer, Kerry Gallagher, D. L Egholm. The Impact of Lithology on Fjord Morphology. Geophysical Research Letters, 2021, 48 (16), pp.e2021GL093101. 10.1029/2021GL093101 . insu-03320558

HAL Id: insu-03320558

https://insu.hal.science/insu-03320558v1

Submitted on 16 Aug 2021

HAL is a multi-disciplinary open access archive for the deposit and dissemination of scientific research documents, whether they are published or not. The documents may come from teaching and research institutions in France or abroad, or from public or private research centers.

L'archive ouverte pluridisciplinaire **HAL**, est destinée au dépôt et à la diffusion de documents scientifiques de niveau recherche, publiés ou non, émanant des établissements d'enseignement et de recherche français ou étrangers, des laboratoires publics ou privés.

Check for updates

Geophysical Research Letters

RESEARCH LETTER
10.1029/2021GL093101

Key Points:

- Observations in East Central Greenland show that lithology controls the width of fjords with softer rocks leading to wider fjords
- Glacial erosion models reproduce the observations with a quarrying law but not when varying the erodibility factor in an abrasion law
- The lithological contribution to glacial erosion law needs more careful description

Supporting Information:

Supporting Information may be found in the online version of this article.

Correspondence to:

M. Bernard,
mabernard.ns@gmail.com

Citation:

Bernard, M., Steer, P., Gallagher, K., & Egholm, D. L. (2021). The impact of lithology on fjord morphology. *Geophysical Research Letters*, *48*, e2021GL093101. https://doi.org/10.1029/2021GL093101

Received 1 MAR 2021
Accepted 23 JUL 2021

© 2021. American Geophysical Union. All Rights Reserved.

The Impact of Lithology on Fjord Morphology

M. Bernard[1], P. Steer[1], K. Gallagher[1], and D. L. Egholm[2]

[1]University of Rennes, CNRS, Rennes, France, [2]Department of Geoscience, Aarhus University, Aarhus, Denmark

Abstract Assessing the impact of glaciations on topography and the co-evolution of ice-sheet dynamics requires a thorough understanding of the factors that control fjord morphology. We investigate the role of lithology on glacial valley form using topographic analyses and numerical landscape evolution models. We measure fjord depths and widths from East Central Greenland (68°N–75°N), and find a control of lithology on fjord width, with wider fjords in softer rocks (i.e., sedimentary rocks). This dependency of fjord width to bedrock properties is predicted by a quarrying erosion law, but not by an abrasion one, when considering results from a simple two-dimensional model and a more detailed three-dimensional ice flow model (iSOSIA). Our analyses and numerical results reveal a potential control of lithology on the width of glacial valleys with glacial quarrying as a plausible responsible mechanism.

Plain Language Summary The present dynamics of the Greenland ice sheet is strongly influenced by fjords, which drain most of the continental ice into the ocean. Fjords are distinct geomorphological features formed by glacial erosion. They have spectacular dimensions with depths greater than 1 km, and width reaching up to 40 km (Scoresby Sund fjord, East Greenland). Understanding the factors that controlled the development of these glacial valleys can enable us to better evaluate the past and future evolution of the ice sheet and its sensitivity to climate change. In East Central Greenland (ECG), fjords show contrasting morphologies at the boundaries between different lithologies. To understand the role of lithology in controlling fjord morphology, we couple quantitative topographic analyses in ECG and numerical modeling of fjord development. We find that lithology controls fjord morphology with softer rocks leading to wider fjords. Next, we show that a classical glacial abrasion erosion law in numerical models does not reproduce the observations in ECG, while a process-based erosion model of rock quarrying by ice does. We therefore advocate that the mechanics of ice erosion, and its sensitivity to lithology, should be considered as a fundamental aspect in the feedbacks between ice-sheet dynamics, topography, and climate change.

1. Introduction

The dynamics and stability of ice sheets are strongly influenced by fjords, which act as major drainage outflow systems for ice (Bennett, 2003). At high latitudes, fjords control the flux of freshwater, nutrients, and sediments to the ocean and impact the dynamics of deltas and offshore sediment deposits (Bendixen et al., 2017). Fjords can have spectacular dimensions with depths up to 1.5 km (e.g., Sognefjord, Norway), and widths larger than 40 km (e.g., Scoresby Sund, Greenland). Determining the controlling factors of fjord development is required to reconstruct or predict the evolution of ice sheets, as the amount of ice drained by fjords strongly depends on their size and morphology. In some regions, fjords display contrasting morphologies at the boundary between different lithologies (Lane et al., 2016; Swift et al., 2008), or along structural weaknesses (Glasser & Ghiglione, 2009; Nesje & Whillans, 1994). However, it is unclear how the erosion processes interact with different lithological properties to produce these variable shapes.

It is well recognized that the pace and mechanics of glacial erosion depend on bedrock properties (Augustinus, 1992a; Boulton, 1979; Kelly et al., 2014; Krabbendam & Glasser, 2011) and fracture density (Becker et al., 2014; Dühnforth et al., 2010). Most numerical models of glacial erosion by abrasion account for this lithological effect through an erodibility factor (Harbor, 1995; Kessler et al., 2008). However, these models fail to reproduce the extreme width of some glacial valleys in Greenland, Antarctica, and Patagonia (Seddik et al., 2009). Indeed, the linear dependence of abrasion laws to erodibility does not capture important non-linear factors relating bedrock resistance to erosion. In contrast, erosion laws describing the removal of rock

fragments by ice, or quarrying, incorporate a nonlinear threshold related to bedrock strength (Hallet, 1996; Iverson, 2012).

Here, we assess the role of lithology in the development of fjord morphology. We first use quantitative morphological analyses in East Central Greenland (ECG) to show that the width distribution of fjords depends on bedrock lithology. Second, we use simple two-dimensional (2D) kinematic models of ice flow to show that a quarrying erosion law, with a threshold on ice velocity (Hallet, 1996; Iverson, 2012), reproduces at first order the observed sensitivity of fjord width to bedrock lithology, while a classically used abrasion law with linear variation of bedrock erodibility factor does not. Last, we use a state-of-the-art ice erosion model (Egholm et al., 2017), that incorporates a quarrying law, to explore the role of rock properties on fjord morphology.

2. Lithological Control on Fjord Width in East Central Greenland

Fjords in ECG (68°N–75°N) show contrasting morphologies coincident with lithological domains (Figure 1a). From west to east, these domains correspond to Archean-early Proterozoic gneisses, late Proterozoic metasediments, Devonian to Cretaceous sedimentary basins with fluvial-lacustrine sediments, sandstones, and marine shales (Figure S1). The southern part of the study area is characterized by Tertiary basaltic lavas and plutons (Henriksen et al., 2000). Based on previous field experiments on rock masses (i.e., uniaxial compressive experiments), Hoek (2001) proposed a classification of rock strength according to their proportion of flaws (i.e., foliation, rounded grains, and fractures). We follow this classification, to evaluate, a priori, the resistance of these lithological domains to erosion. The Proterozoic gneisses and the Late Proterozoic metasediments are considered as hard rocks, which we define here as having a higher resistance to erosion. The Devonian (i.e., terrestrial sediments) to Mesozoic sedimentary rocks (i.e., shallow marine sediments to marine shales) define softer rocks, with a lower resistance to erosion.

Using image processing algorithms, we extract the depth D and width W from fjords valley centers in ECG using a 450 m resolution DEM (Figures 1 and S2; BedMachine v3, Morlighem et al., 2017) that includes sub-glacial bed topography and bathymetry data. We define the valley contours as the intersection between the topography and a horizontal plane located at the local mean elevation (see Supporting Information). We then convert fjord contours into a binary image from which we apply a skeletonization algorithm to extract the fjord centerlines. From valley contours and centerlines, we consider fjord depth as the distance between the minimum elevation along the valley width and the elevation corresponding to the intersection between the topography and the horizontal plane located at the mean elevation of the local topography (see Figure 1b inset). Fjord width corresponds to two times the minimum horizontal distance between the valley center and the valley contour. To compare the distributions of fjord W for different lithologies, we consider drainage area A as a proxy for ice discharge (e.g., Augustinus, 1992b). This in turn reduces the sensitivity of the results to the valley location relative to the main ice flow lines (Figures 1d and S2d). We infer the relationships between W and A by fitting power-law functions to the mean values of binned data. In the following, we only focus on fjords with an elevation below modern sea level, but we have performed a similar analysis on all the glacial valleys (Figure S3).

Fjords in the hard gneissic basement or in the metasediments tend to be deeper and narrower than those in the softer Mesozoic sediments (Figure 1c). Volcanic rocks represent an intermediate case with some basalt-hosted fjords as wide as 25 km and others as deep as 1.5 km. While there is no clear relationship between D and W, W increases with A for all lithologies (Figure 1d). The exponents of the W-A power-laws are higher for the softer sedimentary rocks (0.20 ± 0.01) than for the harder gneisses (0.15 ± 0.01) and metasediments (0.12 ± 0.02, see Table S1). Volcanic rocks have the highest exponent (0.28 ± 0.02), implying rapid fjord widening with increasing A. The layered nature of these basalts with a 10–15° seaward dip (Henriksen et al., 2000) may have enhanced glacial erosion (Kelly et al., 2014). Overall, an inverse relationship seems to characterize the relationship between lithological hardness and D (Figures S2 and S3), but is not as obvious as for fjord W. Our analysis suggests that lithology controls the widening of fjords in ECG, with sedimentary rocks generally associated with wider fjords.

10.1029/2021GL093101

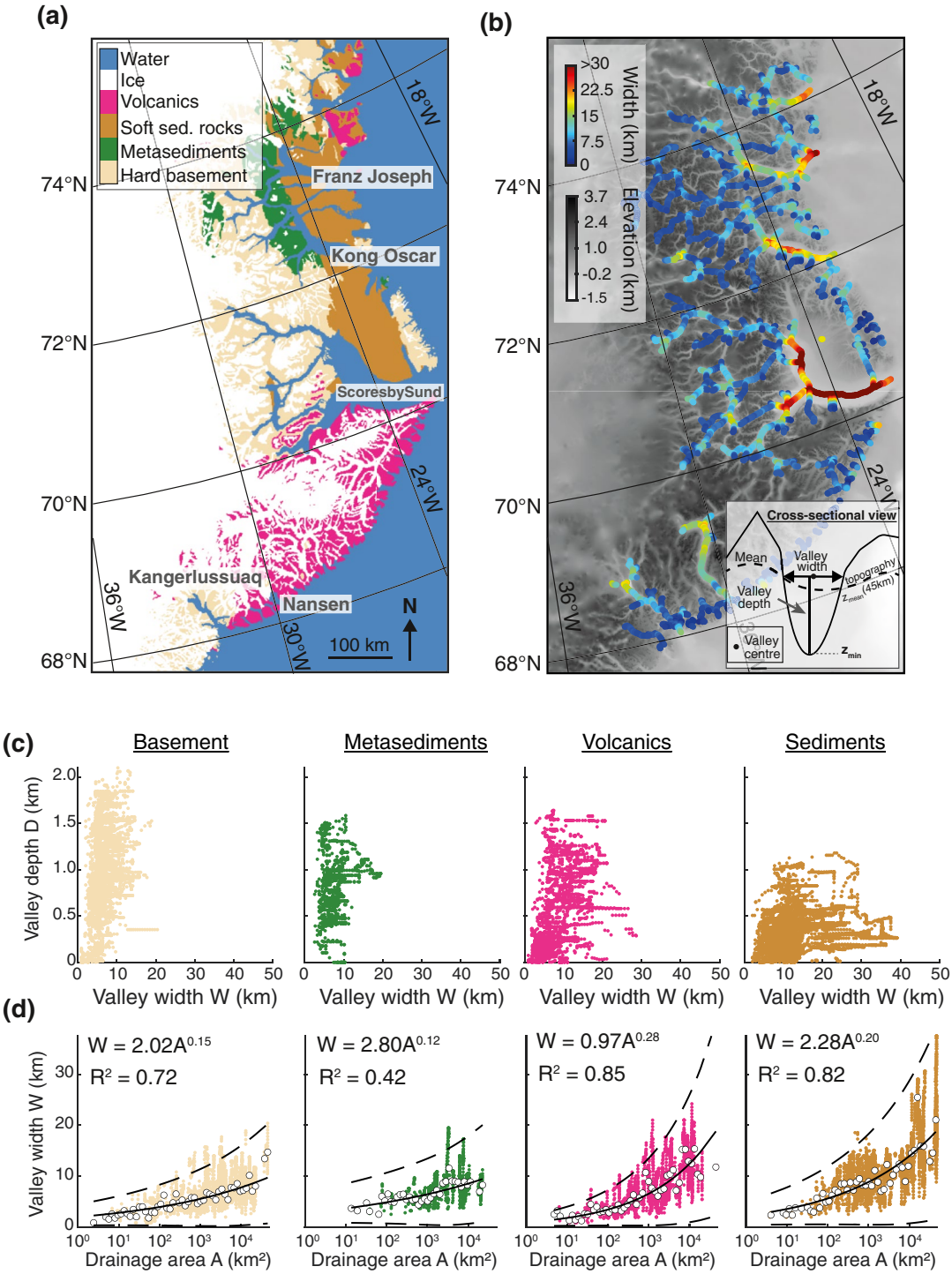

Figure 1. Morphological analyses of fjords in East Central Greenland (68°N–75°N). (a) Main lithological units from the 1:2,500,000 geological map (Henriksen et al., 2000). (b) Widths along fjord centerlines computed according to the method illustrated in the inset. Bed topography is from the BedMachine v3 DEM (Morlighem et al., 2017). (c) Fjord widths are plotted against fjord depths and (d) drainage area according to lithological units. The white circles in (d) are the mean values of binned data.

3. Predicting Fjord Morphology With Simple Kinematic Ice Flow Models

We use simple 2D kinematic models of ice flow to test the ability of three different erosion laws to produce lithology-dependent valley morphologies. The first is an abrasion law with an erosion rate $\dot{E}$ proportional to the square of the basal sliding speed U_b (Herman et al., 2015):

$$\dot{E} = k_1 U_b^2, \tag{1}$$

where k_1 is an erodibility constant (m^{-1} yr) accounting for lithology. The second law considers quarrying in a simplistic manner:

$$\dot{E} = k_1 \left(U_b - U_c\right)^2, \tag{2}$$

by incorporating a threshold U_c on the basal sliding speed, which reflects the minimum velocity required to detach and transport blocks. Threshold-limited erosion laws are classically used to describe fluvial incision (Lague et al., 2005), but we adapt this form here for glacial erosion. The third law (Iverson, 2012) represents quarrying by ice flow over cavities in the lee side of bedrock topographic steps:

$$\dot{E} = k_2 p_f G U_b, \tag{3}$$

where k_2 is a scaling factor, $G = h_c/2L_c\,(1 - S/L_c)$ is a bed geometric factor with h_c the height of bedrock steps (Table S3), and $1 - S/L_c$ the ice-bed contact area defined by the cavity length S, and L_c the distance between bedrock steps. The probability, p_f, that a stressed bedrock step fails is:

$$p_f = 1 - \exp\left(-V_f \left(\frac{\sigma_d}{\omega\sigma_0}\right)^m\right), \tag{4}$$

where V_f is a volume factor, and $\left(\sigma_d \,/\, \omega\sigma_0\right)^m$ is a differential stress factor accounting for the deviatoric stress σ_d on the bedrock step given a bedrock strength heterogeneity m (Ugelvig et al., 2018). The critical stress σ_0 represents the tensile strength of the rock, scaled by a factor ω to account for slow subglacial crack growth under smaller stresses (Iverson, 2012). The probability of failure p_f is the best proxy for bedrock strength or erodibility, in this model. Neglecting the volume factor ($V_f = 1$), p_f is to first order close to 1 when $\sigma_d \,/\, \omega\sigma_0 > 1$, and decreases rapidly when $\sigma_d \,/\, \omega\sigma_0$ tends toward 0, with m controlling the rate of decrease (Figure S4). When m tends toward infinity, this model becomes equivalent to a threshold model, but with a threshold defined on deviatoric stress $\sigma_d = \omega\sigma_0$, rather than sliding speed.

We apply these models to an initial V-shaped valley with ice velocity defined as a power-law function of shear stress and effective pressure (Equation S4), and the effect of valley curvature on ice dynamics included (see Supporting Information). During the simulation, we keep the initial ice elevation constant and equal to the maximum elevation in the valley (751 m). The models were stopped when the valley reached a depth of ~1 km (Figure 2). The abrasion law (Equation 1) produces the same valley morphology irrespective of the erodibility coefficient k_1, which simply scales the duration of the simulation (Figure 2 and Table S3). The threshold model (Equation 2) promotes the narrowing of the valley, as U_c limits erosion of the valley walls where U_b is low (Figure 2b and Table S3). We then consider two models using the quarrying law (Equation 3) and representing soft (M_1) and hard (M_2) lithologies. This law predicts a large range of fjord morphologies and widths according to the bedrock parameters m and σ_0 (Figure 2 and Table S3), and the largest fjords of all our simulations are obtained with the quarrying law with soft rocks. In this law, widening is promoted by relaxing the deviatoric stress and ice sliding speed from which significant erosion occurs (Figure S6). In contrast to this quarrying law, abrasion laws with variable erodibility are inadequate to simulate the observed sensitivity of fjord width to lithology.

4. Assessing Lithological Controls With iSOSIA

To account for potential feedbacks between lithology, fjord morphology, and ice flow, we use a state-of-the-art fjord model (Egholm et al., 2017; iSOSIA), in which a 1 km thick ice sheet flows on an initial fluvial topography. However, we adapt the formulation of the hydrological model in Egholm et al. (2017) to account for steady-state cavitation, where the spacing between the bed steps is constant L_c and the height of cavities

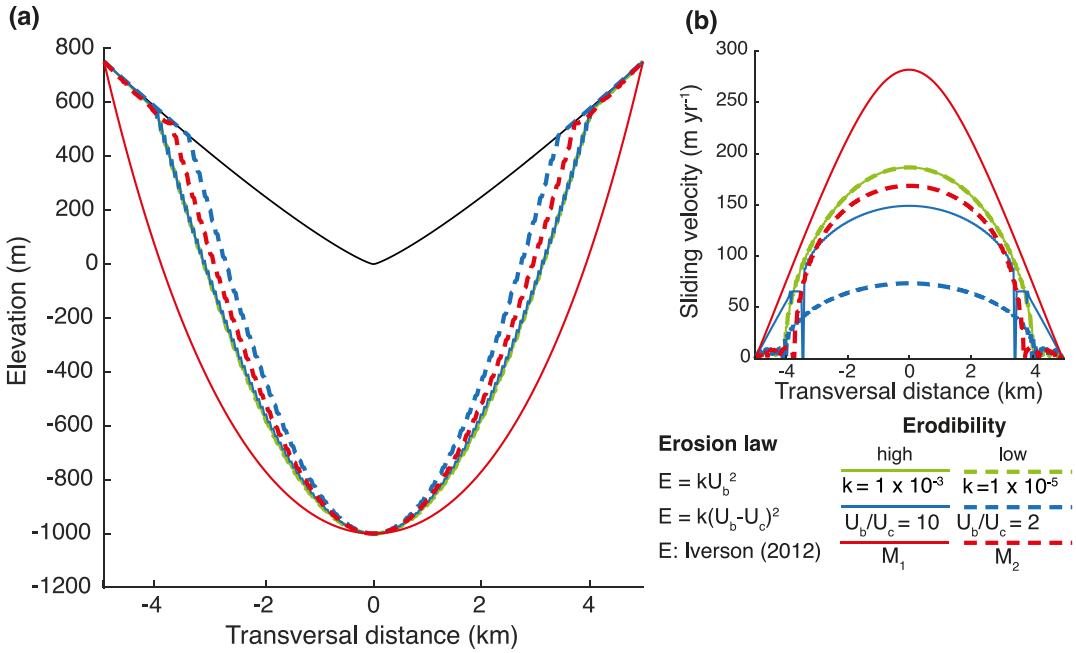

Figure 2. Kinematic models of glacial erosion laws. (a) Fjord valley morphologies at the end of simulations using the three glacial erosion laws defined in the main text. (b) Sliding velocity profiles across the valley transect at the end of the simulation. Some instabilities occur due to sharp curvature at the top of the valley. M_1 and M_2 refer to models 1 and 2, which consider different combinations of parameters σ_0 and m in Equation 4 (Table S3). Note that the blue and green solid lines, as well as the green dashed lines, are almost identical.

on their lee side is a function of bed slope (see Supporting Information). We keep the hydrological model simple and define the water flux as equal to 10% of the local ice flux everywhere across the model. We consider two end-member models of low and high bedrock strength, with variations of σ_0 and m in Equation 4 (Table S4). The range of m is constrained from 1.5 to 5 in natural rocks (Lobo-Guerrero & Vallejo, 2006; Wong et al., 2006), and is not expected to vary with scale (Wong et al., 2006). However, the value of σ_0 is expected to vary greatly with rock cohesion and the scale of the stressed rocks (Hallet, 1996; Lobo-Guerrero & Vallejo, 2006). We thus consider values of σ_0 ranging from 0.1 to 10 MPa. We stop the models when valley incision reaches ~1.3 km in the downstream part of the models.

Results show that fjord width decreases with bedrock strength (Figure 3). For low bedrock strength Equation 4 predicts uniform failure probability p_f across the landscape (Figure S4), as small levels of deviatoric stress, σ_d, are sufficient to dislodge rock fragments. Erosion rate becomes proportional to U_b leading to distributed erosion and fjords widening with a mean of ~16 km and a range of 8–30 km (Figure 3d). However, for higher bedrock strength, a higher σ_d is required to erode, leading in turn to steep gradients in the failure probability (Figure S4). Erosion becomes focused in the central part of fjords, where ice basal sliding speed is maximum, leading to valley deepening rather than widening (Figure 3a). The resulting valley widths are ~11 km on average, with a range of 8–15 km (Figure 3d). For similar depths, the fjords are wider for soft rocks (Figure 3d), consistent with observations in ECG (Figure 1).

Considering high bedrock strength but varying the internal heterogeneity of the rock mass through m (Table S4) also leads to fjord widening when heterogeneity increases or m decreases (Figure S9). This occurs because, as σ_d / $\omega\sigma_0$ is lower along the valley walls, the probability p_f of exploiting well-oriented rock defects is higher when m decreases. This ultimately increases the range of σ_d for which significant erosion will occur (Figure S4). Moreover, topographic relief can also control fjord morphologies by confining a glacier into deep valleys (Kessler et al., 2008). We therefore vary the initial relief from 1,500 to 500 m. For all the iSOSIA quarrying-based models we observe a similar dependence of fjord width to lithology/bedrock strength (Figures S10 and S11). In contrast, abrasion-based models, lead to no significant morphological change (Figures 3e–3h), when varying the erodibility constant (Table S4).

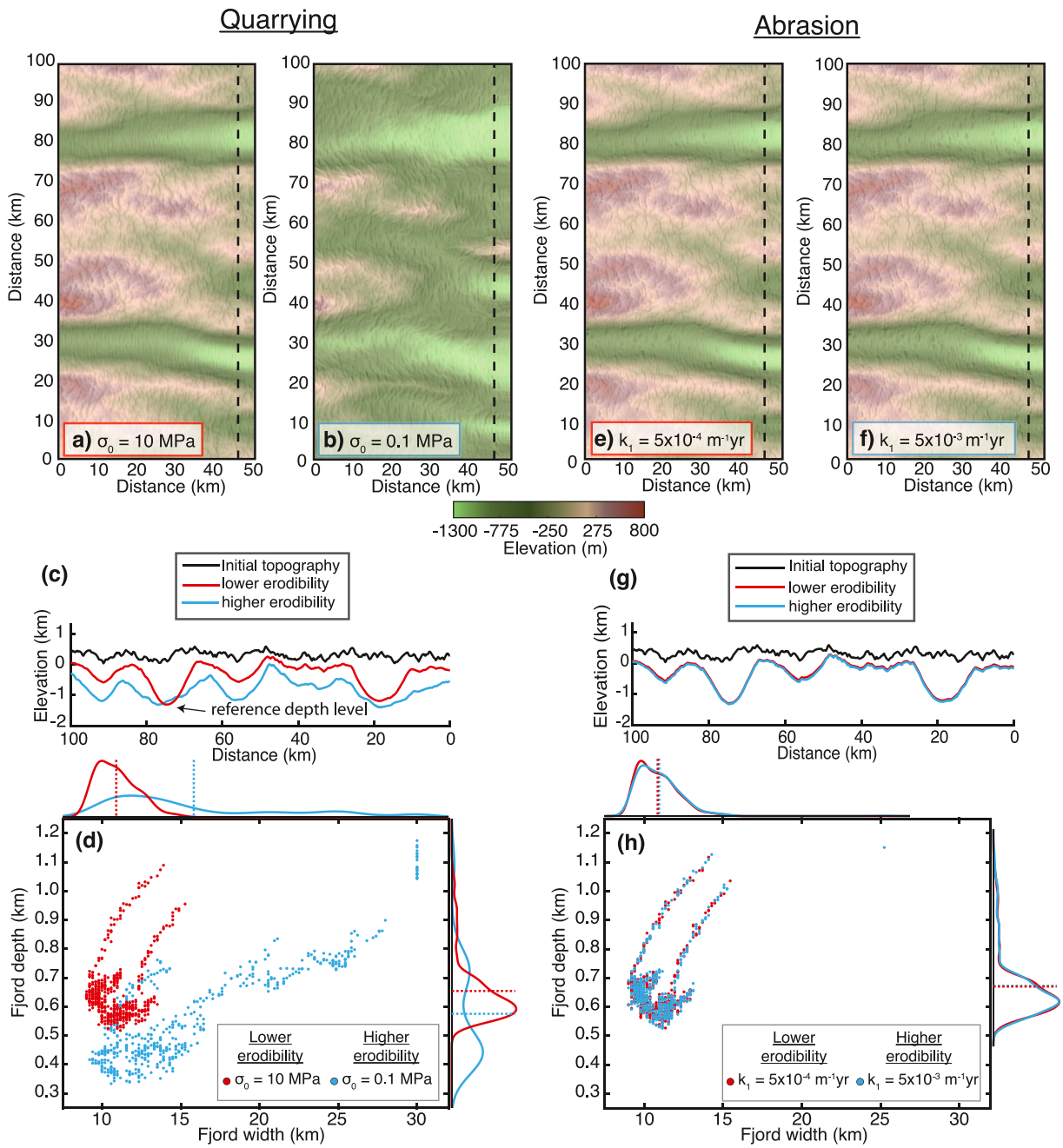

Figure 3. iSOSIA fjord models considering various bedrock erodibility with quarrying and abrasion laws. (a and b) Erodibility is set by varying σ_0 for quarrying (Equation 4) and (e and f) varying by an order of magnitude k_1 for abrasion (Equation 1). (c and g) Cross-sectional views of the resulting fjords shown along one transect downstream. (d and h) Fjord widths against depths for the respective models. The marginal distributions for width and depth are shown, with dashed lines corresponding to the mean of each distribution with similar colors. The parameter m (Equation 4) is kept constant ($m = 2.7$).

5. Discussion

We evaluated the role of lithology on the fjord morphologies in ECG, by analyzing their depths and widths. The scaling between fjord width and drainage area (or ice discharge) varies with lithology, with broader valleys associated with softer rocks (i.e., sedimentary rocks); consistent with previous observations (Swift et al., 2008). The influence of lithology on fjord morphology has also been described for a variety of lithologies in West Greenland (Lane et al., 2016), Iceland (Brook et al., 2004), Scotland (Brook et al., 2004; Krabbendam & Glasser, 2011), New-Zealand (Augustinus, 1992a), Norway (Nesje & Whillans, 1994), and Patagonia (Glasser

& Ghiglione, 2009), thus supporting our results. To test whether our results strongly depend on the reference elevation, we performed the same morphological analyses but considering sea-level as an absolute reference elevation from where to measure fjord width and depth following Augustinus (1992b). Overall, results show a similar, and even higher, sensitivity of fjord width to ice discharge variations for the softer sedimentary covers (exponent of 0.29 ± 0.03) compared to the harder gneisses (exponent of 0.13 ± 0.02, see Figure S12 and Table S5), further supporting the potential lithological control on fjord width. Extending our analysis to all glacial valleys also leads to a clear correlation between fjord width scaling and lithology (Figure S3).

However, other processes could also influence valley widening. In ECG, the resulting fjord morphology may be partly inherited from the pre-glacial topography, which steers ice flow and controls the pattern of glacial erosion (Kessler et al., 2008; Pedersen et al., 2014). Indeed, initially high elevation in the interior is likely to have confined glacial erosion within valleys (promoting deepening) while lower relief toward the coast enables the ice to flow over larger areas and to widen the valleys. However, erosion histories deduced from both low-temperature thermochronology (Bernard et al., 2016) and isostatic reconstitution (Pedersen et al., 2019) suggest that fjord incision in ECG started before 2.5 Ma and propagated inland, with potentially similar total erosion. Following Swift et al. (2008), our results suggest this morphological difference may have rather been favored by a combination of difference of initial relief and of resistance to erosion (Figures S10 and S11).

Fjord width can also be influenced by fluvial and hillslope erosion. This would imply that differences in hillslope dynamics and sediment valley filling between the still-glaciated inner parts and the partly deglaciated outer parts of the fjords could influence our results. We foresee two possible contrasting cases: (a) fjords developed in fluvially dissected landscapes, where topographic crests delimit the maximum extent of a valley; or (b) fjords bounded by low relief surfaces. In the first case, landscape evolution models of non-glaciated landscapes show that valley width does not evolve significantly under subaerial hillslope processes after the cessation of vertical incision (e.g., Egholm et al., 2013). Valleys are strictly bounded by crests which horizontal motion is set by the difference of erosion rates on the two sides of the crest. In this case, we do not expect subaerial hillslope processes to have a large influence on valley width. In the second case, cessation of incision and glacial retreat will leave the lateral walls of the fjord exposed to subaerial hillslope processes. Steep slopes will be exposed mainly to gravitational mass wasting processes (e.g., landsliding) that will reduce the slope and progressively lead to other dominant hillslope process, including periglacial frost cracking or soil creep (Hales & Roering, 2009; Roering et al., 1999, 2001). In any case, valley widening by these processes cannot be of an amplitude much greater than the approximate height of the valley wall, as hillslope erosion efficiency decreases rapidly and nonlinearly with slope (e.g., Roering et al., 1999). Moreover, the response time of hillslope erosion after glacier retreat has been suggested to depend on lithology (Augustinus, 1992a, 1995). Finally, valleys greater than 10 kilometers width, as in the downstream part of the Scoresby Sund (>40 km), are only found in the glacial environment on Earth. This correlation further suggests that the subaerial process alone cannot be responsible for valley widening. We therefore advocate that a glaciological explanation of this lithologically controlled widening is reasonable through the process of glacial quarrying, which allows for the slower ice sliding speed found close to the valley walls to detach rock fragments and significantly erode laterally. Finally, fluvial erosion occurring during interglacial periods and potentially accelerated by megaflood events during glacier retreat (Keisling et al., 2020) have also possibly amplified fjord incision.

Our modeling results demonstrate that predicted fjord width depends on lithology only when considering erosion laws with thresholds on the ice's basal sliding speed or deviatoric stress. This nonlinear behavior naturally emerges with a quarrying law (Iverson, 2012), leading to a mechanical basis for the lithological dependency, accounted for by the bulk rock strength σ_0 and the rock defect density described by m (Equation 4). This is consistent with previous studies suggesting that bedrock resistance to erosion is determined through rock mass strength (Augustinus, 1992a; Brook et al., 2004), lithological and structural properties, including grain size (Wong et al., 2006), foliations (Lobo-Guerrero & Vallejo, 2006), densities of flaws and fractures (Becker et al., 2014; Dühnforth et al., 2010). Despite that, most landscape evolution models consider glacial erosion through an abrasion law where erosion rate is proportional to erodibility. Due to this linear relationship, an abrasion law unsurprisingly fails to predict any dependency of fjord width to lithology. Yet, this may suggest that quarrying is the main mechanism by which fjords widen in natural settings where

both abrasion and quarrying act simultaneously; or that the considered abrasion law lacks physical ingredients. Indeed, we note that the abrasion mechanism could show a lithological dependency if other factors such as debris concentration (Boulton, 1979; Hallet, 1979), debris hardness (Hallet, 1979) and porosity (Lee & Rutter, 2004) are included. In fact, abrasion and quarrying are two closely linked erosion processes, as the tools for abrasion are typically provided by quarrying. Hence, factors that scale rates of quarrying must also, by the availability of tools, influence the rates of abrasion (Ugelvig & Egholm, 2018).

We suggest that modified abrasion-type laws could encompass a nonlinear dependency on lithology by considering a variable exponent, and could be used as a more simple formalism for quarrying. Indeed, we successfully fitted ($R^2 = 0.83$–0.96) abrasion-type power laws between erosion rate and sliding speed for results obtained with our quarrying law models (Figure S13). Keeping m equal to 2.7, we find that the power-law exponent increases from 1.0 to 2.0 when σ_0 increases from 0.1 to 10 MPa. Increasing m to 4.2, while keeping $\sigma_0 = 10$ MPa, even leads to an exponent of 2.5. In other words, decreasing rock resistance could be accounted for in abrasion-type laws by increasing the pre-exponent factor, but also decreasing the exponent, as also suggested by Iverson (2012). This demonstrates that the dependency of erosion rates on lithology is not only a matter of eroding faster or slower through an erodibility constant but also reflects changes in the spatial distribution of erosion relative to ice flow. This modified abrasion-type law also provides a simple formalism to account for quarrying and lithological controls on fjord morphology in numerical models. Nevertheless, as recently suggested (Herman et al., 2021), glacial landforms are the results of the interactions between glacial abrasion, quarrying, and fluvial transport of sediments, which act as combined systems. Therefore, future modeling approaches should focus on investigating the importance of this coupling in terms of resulting glacial valley morphology.

6. Conclusion

To conclude, our study suggests that lithology, and more specifically rock strength and the density of mechanical heterogeneities, influence the morphology of glacial valleys by favoring the development of wide valleys in soft rocks and narrower valleys in harder rocks. This is supported by quantitative observations in ECG and by modeling results that couple ice dynamics to erosion by quarrying. Yet, we acknowledge that valley widening in ECG could have been favored by geomorphological processes other than those considered in our modeling approach, including hillslope processes. Our modeling results also show that a classically used abrasion law cannot explain the sensitivity of fjord width to lithology. This in turn implies either that the classical abrasion law is lacking some physical ingredients to relate lithology and abrasion rates, or that quarrying is the dominant process controlling the morphology of glacial valleys. In nature, bedrock properties also set the relative proportion of abrasion and quarrying acting on the bed (Becker et al., 2014; Kelly et al., 2014; Krabbendam & Glasser, 2011), but possibly with different responses to ice dynamics and with different implications for valley morphology. We therefore advocate that the mechanics of ice erosion, and its sensitivity to lithology, should be considered as a fundamental aspect in the feedbacks between ice sheet or glacier dynamics, topography, and climate change (Herman et al., 2021; Kessler et al., 2008; Pedersen & Egholm, 2013; Steer et al., 2012).

Data Availability Statement

The DEM (BedMachine v3) used in this study can be downloaded here: BedMachine Greenland v3| Ice Sheet Modeling Group (uci.edu). The code used to extract the fjord widths and depths are also available at https://doi.org/10.5281/zenodo.4888958 (Bernard, 2021) (GNU license). The iSOSIA version 3.3.8c used in this study are available here: https://doi.org/10.5281/zenodo.4568845 (Egholm, 2021) (GNU license).

Acknowledgments
The authors acknowledge the University of Rennes 1, the University of Aarhus, the European Research Council and the Denmark French Institute for having funded this study. The authors also thank J. Braun, P. Valla, P. Van der Beek, C. Gautheron, and C. Colleps for their comments during the preparation of this manuscript.

References

Augustinus, P. C. (1992a). The influence of rock mass strength on glacial valley cross-profile morphometry: A case study from the Southern Alps, New Zealand. *Earth Surface Processes and Landforms*, *17*(1), 39–51. https://doi.org/10.1002/esp.3290170104

Augustinus, P. C. (1992b). Outlet glacier trough size-drainage area relationships, Fiordland, New Zealand. *Geomorphology*, *4*(5), 347–361. https://doi.org/10.1016/0169-555X(92)90028-M

Augustinus, P. C. (1995). Glacial valley cross-profile development: The influence of in situ rock stress and rock mass strength, with examples from the Southern Alps, New Zealand. *Geomorphology*, *14*(2), 87–97. https://doi.org/10.1016/0169-555X(95)00050-X

Becker, R. A., Tikoff, B., Riley, P. R., & Iverson, N. R. (2014). Preexisting fractures and the formation of an iconic American landscape: Tuolumne Meadows, Yosemite National Park, USA. *Geological Society of America Today*, *24*(11), 4–10. https://doi.org/10.1130/GSATG203A.1

Bendixen, M., Lønsmann Iversen, L., Anker Bjørk, A., Elberling, B., Westergaard-Nielsen, A., Overeem, I., et al. (2017). Delta progradation in Greenland driven by increasing glacial mass loss. *Nature*, *550*(7674), 101–104. https://doi.org/10.1038/nature23873

Bennett, M. R. (2003). Ice streams as the arteries of an ice sheet: Their mechanics, stability and significance. *Earth-Science Reviews*, *61*(3–4), 309–339. https://doi.org/10.1016/S0012-8252(02)00130-7

Bernard, M. (2021). *MBernAca/MorphoECG: MorphoECG v1.0 (version 1.0)*. Zenodo. https://doi.org/10.5281/zenodo.4888958

Bernard, T., Steer, P., Gallagher, K., Szulc, A., Whitham, A., & Johnson, C. (2016). Evidence for Eocene-Oligocene glaciation in the landscape of the east Greenland margin. *Geology*, *44*(11), 895–898. https://doi.org/10.1130/G38248.1

Boulton, G. S. (1979). Processes of glacier erosion on different substrata. *Journal of Glaciology*, *23*(89), 15–38. https://doi.org/10.3189/S0022143000029713

Brook, M. S., Kirkbride, M. P., & Brock, B. W. (2004). Rock strength and development of glacial valley morphology in the Scottish Highlands and northwest Iceland. *Geografiska Annaler—Series A: Physical Geography*, *86*(3), 225–234. https://doi.org/10.1111/j.0435-3676.2004.00227.x

Dühnforth, M., Anderson, R. S., Ward, D., & Stock, G. M. (2010). Bedrock fracture control of glacial erosion processes and rates. *Geology*, *38*(5), 423–426. https://doi.org/10.1130/G30576.1

Egholm, D. L. (2021). *davidlundbek/iSOSIA: spm-3.3.8c* (version v3.3.8c). Zenodo. https://doi.org/10.5281/zenodo.4568845

Egholm, D. L., Jansen, J. D., Brædstrup, C. F., Pedersen, V. K., Andersen, J. L., Ugelvig, S. V., et al. (2017). Formation of plateau landscapes on glaciated continental margins. *Nature Geoscience*, *10*(8), 592–597. https://doi.org/10.1038/NGEO2980

Egholm, D. L., Knudsen, M. F., & Sandiford, M. (2013). Lifespan of mountain ranges scaled by feedbacks between landsliding and erosion by rivers. *Nature*, *498*(7455), 475–478. https://doi.org/10.1038/nature12218

Glasser, N. F., & Ghiglione, M. C. (2009). Structural, tectonic and glaciological controls on the evolution of fjord landscapes. *Geomorphology*, *105*(3–4), 291–302. https://doi.org/10.1016/j.geomorph.2008.10.007

Hales, T. C., & Roering, J. J. (2009). A frost "buzzsaw" mechanism for erosion of the eastern Southern Alps, New Zealand. *Geomorphology*, *107*(3), 241–253. https://doi.org/10.1016/j.geomorph.2008.12.012

Hallet, B. (1979). A theoretical model of glacial abrasion. *Journal of Glaciology*, *23*(89), 39–50. https://doi.org/10.3189/S0022143000029725

Hallet, B. (1996). Glacial quarrying: A simple theoretical model. *Annals of Glaciology*, *22*, 1–8. https://doi.org/10.1017/s0260305500015147

Harbor, J. M. (1995). Development of glacial-valley cross sections under conditions of spatially variable resistance to erosion. *Geomorphology*, *14*(2), 99–107. https://doi.org/10.1016/0169-555X(95)00051-1

Henriksen, N., Higgins, A. K., Kalsbeek, F., & Pulvertaft, T. C. R. (2000). Greenland from Archaean to Quaternary. Descriptive text to the geological map of Greenland, 1: 2,500,000. *Geology of Greenland Survey Bulletin*, *185*, 2–93. https://doi.org/10.34194/ggub.v185.5197

Herman, F., Beyssac, O., Brughelli, M., Lane, S. N., Leprince, S., Adatte, T., et al. (2015). Erosion by an Alpine glacier. *Science*, *350*(6257), 193–195. https://doi.org/10.1126/science.aab2386

Herman, F., De Doncker, F., Delaney, I., Prasicek, G., & Koppes, M. (2021). The impact of glaciers on mountain erosion. *Nature Reviews Earth & Environment*, *2*, 422–435. https://doi.org/10.1038/s43017-021-00165-9

Hoek, E. (2001). Rock mass properties for underground mines. In W. A. Hustrulid, & R. C. Bullock (Eds.), (Eds), *Underground mining methods: Engineering fundamentals and international case studies* (Vol. 21). SME.

Iverson, N. R. (2012). A theory of glacial quarrying for landscape evolution models. *Geology*, *40*(8), 679–682. https://doi.org/10.1130/G33079.1

Keisling, B. A., Nielsen, L. T., Hvidberg, C. S., Nuterman, R., & DeConto, R. M. (2020). Pliocene-Pleistocene megafloods as a mechanism for Greenlandic megacanyon formation. *Geology*, *48*(7), 737–741. https://doi.org/10.1130/G47253.1

Kelly, M. H., Anders, A. M., & Mitchell, S. G. (2014). Influence of bedding dip on glacial erosional landforms, Uinta mountains, USA. *Geografiska Annaler—Series A: Physical Geography*, *96*(2), 147–159. https://doi.org/10.1111/geoa.12037

Kessler, M. A., Anderson, R. S., & Briner, J. P. (2008). Fjord insertion into continental margins driven by topographic steering of ice. *Nature Geoscience*, *1*(6), 365–369. https://doi.org/10.1038/ngeo201

Krabbendam, M., & Glasser, N. F. (2011). Glacial erosion and bedrock properties in NW Scotland: Abrasion and plucking, hardness and joint spacing. *Geomorphology*, *130*(3–4), 374–383. https://doi.org/10.1016/j.geomorph.2011.04.022

Lague, D., Hovius, N., & Davy, P. (2005). Discharge, discharge variability, and the bedrock channel profile. *Journal of Geophysical Research*, *110*(4), F04006. https://doi.org/10.1029/2004JF000259

Lane, T. P., Roberts, D. H., Cofaigh, C. O., Rea, B. R., & Vieli, A. (2016). Glacial landscape evolution in the Uummannaq region, West Greenland. *Boreas*. *45*, 220–234. https://doi.org/10.1111/bor.12150

Lee, A. G. G., & Rutter, E. H. (2004). Experimental rock-on-rock frictional wear: Application to subglacial abrasion. *Journal of Geophysical Research*, *109*(9), B09202. https://doi.org/10.1029/2004JB003059

Lobo-Guerrero, S., & Vallejo, L. E. (2006). Application of Weibull statistics to the tensile strength of rock aggregates.*Journal of Geotechnical and Geoenvironmental Engineering*, *132*, 786–790. https://doi.org/10.1061/(asce)1090-0241(2006)132:6(786)

Morlighem, M., Williams, C. N., Rignot, E., An, L., Arndt, J. E., Bamber, J. L., et al. (2017). BedMachine v3: Complete bed topography and ocean bathymetry mapping of Greenland from multibeam echo sounding combined with mass conservation. *Geophysical Research Letters*, *44*(21), 11051–11061. https://doi.org/10.1002/2017GL074954

Nesje, A., & Whillans, I. M. (1994). Erosion of Sognefjord, Norway. *Geomorphology*, *9*, 33–45. https://doi.org/10.1016/0169-555x(94)90029-9

Pedersen, V. K., & Egholm, D. L. (2013). Glaciations in response to climate variations preconditioned by evolving topography. *Nature*, *493*(7431), 206–210. https://doi.org/10.1038/nature11786

Pedersen, V. K., Huismans, R. S., Herman, F., & Egholm, D. L. (2014). Controls of initial topography on temporal and spatial patterns of glacial erosion. *Geomorphology*, *223*, 96–116. https://doi.org/10.1016/j.geomorph.2014.06.028

Pedersen, V. K., Larsen, N. K., & Egholm, D. L. (2019). The timing of fjord formation and early glaciations in North and Northeast Greenland. *Geology*, *47*(7), 682–686. https://doi.org/10.1130/G46064.1

Roering, J. J., Kirchner, J. W., & Dietrich, W. E. (1999). Evidence for nonlinear, diffusive sediment transport on hillslopes and implications for landscape morphology. *Water Resources Research*, *35*(3), 853–870. https://doi.org/10.1029/1998WR900090

Roering, J. J., Kirchner, J. W., & Dietrich, W. E. (2001). Hillslope evolution by nonlinear, slope-dependent transport: Steady state morphology and equilibrium adjustment timescales. *Journal of Geophysical Research*, *106*(B8), 16499–16513. https://doi.org/10.1029/2001JB000323

Seddik, H., Greve, R., Sugiyama, S., & Naruse, R. (2009). *Numerical simulation of the evolution of glacial valley cross sections* (pp. 1–14). Retrieved from http://arxiv.org/abs/0901.1177

Steer, P., Huismans, R. S., Valla, P. G., Gac, S., & Herman, F. (2012). Bimodal Plio-Quaternary glacial erosion of fjords and low-relief surfaces in Scandinavia. *Nature Geoscience*, *5*(9), 635–639. https://doi.org/10.1038/ngeo1549

Swift, D. A., Persano, C., Stuart, F. M., Gallagher, K., & Whitham, A. (2008). A reassessment of the role of ice sheet glaciation in the long-term evolution of the east Greenland fjord region. *Geomorphology*, *97*(1–2), 109–125. https://doi.org/10.1016/j.geomorph.2007.02.048

Ugelvig, S. V., & Egholm, D. L. (2018). The influence of basal-ice debris on patterns and rates of glacial erosion. *Earth and Planetary Science Letters*, *490*, 110–121. https://doi.org/10.1016/j.epsl.2018.03.022

Ugelvig, S. V., Egholm, D. L., Anderson, R. S., & Iverson, N. R. (2018). Glacial erosion driven by variations in meltwater drainage. *Journal of Geophysical Research: Earth Surface*, *123*(11), 2863–2877. https://doi.org/10.1029/2018JF004680

Wong, T. F., Wong, R. H. C., Chau, K. T., & Tang, C. A. (2006). Microcrack statistics, Weibull distribution and micromechanical modeling of compressive failure in rock. *Mechanics of Materials*, *38*(7), 664–681. https://doi.org/10.1016/j.mechmat.2005.12.002

References From the Supporting Information

Anderson, R. S. (2014). Evolution of lumpy glacial landscapes. *Geology*, *42*(8), 679–682. https://doi.org/10.1130/G35537.1

Braun, J., Zwartz, D., & Tomkin, J. H. (1999). A new surface-processes model combining glacial and fluvial erosion. *Annals of Glaciology*, *28*, 282–290. https://doi.org/10.3189/172756499781821797

Budd, W. F., Keage, P. L., & Blundy, N. A. (1979). Empirical studies of ice sliding. *Journal of Glaciology*, *23*(89), 157–170. https://doi.org/10.3189/S0022143000029804

Egholm, D. L., Knudsen, M. F., Clark, C. D., & Lesemann, J. E. (2011). Modeling the flow of glaciers in steep terrains: The integrated second-order shallow ice approximation (iSOSIA). *Journal of Geophysical Research*, *116*(2), 1–16. https://doi.org/10.1029/2010JF001900

Iverson, N. R., & Petersen, B. B. (2011). A new laboratory device for study of subglacial processes: First results on ice-bed separation during sliding. *Journal of Glaciology*, *57*(206), 1135–1146. https://doi.org/10.3189/002214311798843458

Jamieson, S. S. R., Hulton, N. R. J., & Hagdorn, M. (2008). Modelling landscape evolution under ice sheets. *Geomorphology*, *97*(1–2), 91–108. https://doi.org/10.1016/j.geomorph.2007.02.047

Kamb, B. (1987). Glacier surge mechanism based on linked cavity configuration of the basal water conduit system. *Journal of Geophysical Research*, *92*(B9), 9083–9100. https://doi.org/10.1029/JB092iB09p09083

Larsen, H. C., & Marcussen, C. (1992). Sill-intrusion, flood basalt emplacement and deep crustal structure of the Scoresby Sund region, East Greenland. *Geological Society Special Publication*, *68*(68), 365–386. https://doi.org/10.1144/GSL.SP.1992.068.01.23

Schoof, C. (2010). Ice-sheet acceleration driven by melt supply variability. *Nature*, *468*(7325), 803–806. https://doi.org/10.1038/nature09618

Schwanghart, W., & Scherler, D. (2014). Short Communication: TopoToolbox 2—MATLAB-based software for topographic analysis and modeling in Earth surface sciences. *Earth Surface Dynamics*, *2*(1), 1–7. https://doi.org/10.5194/esurf-2-1-2014